Case Studies in Mechanical Systems and Signal Processing 4 (2016) 8–18

Contents lists available at ScienceDirect

Case Studies in Mechanical Systems and Signal Processing

journal homepage: www.elsevier.com/locate/csmssp

A smart experimental setup for vibration measurement and imbalance fault detection in rotating machinery

Guilherme Kenji Yamamoto, Cesar da Costa*, João Sinohara da Silva Sousa

Control and Automation Engineering, IFSP-Federal Institute of Education, SP, 01109-010, Brazil

ARTICLE INFO

Article history:
Received 20 May 2016
Received in revised form 12 July 2016
Accepted 18 July 2016
Available online 30 July 2016

ABSTRACT

Rotor imbalance is the most common cause of machine vibration. In practice, rotors can never be balanced perfectly owing to manufacturing errors such as porosity in casting, non-uniform density of materials, manufacturing tolerances, and gain or loss of material during operation. Mass imbalance leads to the generation of a centrifugal force, which must be counteracted by bearings and support structures. A full spectrum analysis is presented for vibration signal to reveal the fault specific whirl signatures. The results clearly indicate the potential and feasibility of the discussed approach for the rotor imbalance diagnosis in a rotor shaft system coupled with a three phase induction motor. This paper presents a smart experimental method for vibration measurement and imbalance fault detection in rotating machinery.

1. Introduction

Rotor balancing is required on all types of rotating machinery, including motors, to ensure smooth machine operation. In a factory, this is achieved on a balancing machine at a precision level determined by motor speed, size, and vibration requirements. The highest precision is required for two-pole motors. Two-pole and large four-pole motors should be balanced at their operating speed in the balancing machine. The assembled motors are then tested to confirm that the vibration requirements are met in operation. Although they do not usually directly concern users, a few salient factors affecting factory balancing, mainly pertaining to two-pole motors, will be discussed here. Most medium-to-large motors are used for constant-speed applications, although there has been a recent increase in the number and size of motors used for variable-speed applications with adjustable-speed drives. Constant-speed motors need to be precision-balanced only at one speed, namely, the operating speed. Variable speed applications require that good rotor balance be maintained throughout the operating speed range, which may typically range from 40% to 100% of their synchronous speed [1–3].

Rotor balancing involves the entire rotor structure, which is made up of a multitude of parts, including the shaft, rotor laminations, end heads, rotor bars, end connectors, retaining rings (where required), and fans. The design and manufacture of these components must be controlled for achieving stable precision balance. Specifically, the following must be taken into account: (i) parts must be precision manufactured to ensure close concentricities and to minimize individual imbalance; (ii) loose parts, which can result in shifting during operation, leading to a change in balance, must be avoided or minimized; and (iii) balance correction weights should be added at or near points of imbalance [4,5].

* Corresponding author.
E-mail addresses: guilhermekenji@yahoo.com.br (G.K. Yamamoto), ccosta@ifsp.edu.br (C. da Costa), sinohara@uol.com.br (J.S. da Silva Sousa).

http://dx.doi.org/10.1016/j.csmssp.2016.07.001

Rotor imbalance generates reaction force in the coupling, which is often a major cause of vibration in machinery. Szabo [6] first evaluated the unbalanced forces generated in a rotor shaft and showed the presence of first (x1) and second (2x) levels of harmonic vibration responses. Different methodologies based on vibration spectral analysis have been proposed using fast Fourier transform (FFT) [7,8]. Bossio et al. [9] studied angular misalignment and imbalance in induction motors with flexible couplings. Tallam et al. [10] investigated load imbalance and shaft misalignment using stator current in inverter-driven induction motors. Martinez-Morales et al. [14] analyzed imbalance and misalignment by using data fusion for multiple mechanical fault diagnosis in induction motors. Quiao et al. [15] reported that imbalance faults constitute a significant portion of all faults in wind turbine generators (WTGs). Historically, vibration-monitoring techniques have been used widely for diagnosing imbalance faults in induction motors, but as reported by Kucuker et al. [16,17], electrical detection methods have been preferred in recent years [18].

In this work, we develop a smart experimental setup with a field programmable gate array (FPGA)-based signal processor that uses a parallel architecture for multiple-signal processing to combine vibration and FFT analysis.

2. Vibrations of rotating machines

A vibration is the movement of a physical quantity in relation to a reference location in a cyclically increasing and decreasing manner as a function of time. The most important features of machine vibration change according to Equation 1. Fig. 1 shows the behavior of Equation 1 in the time domain [6].

$$x(t) = Asen(wt + \phi) \tag{1}$$

where

A: amplitude (m/s);
w: angular frequency (rad/s);
ϕ: initial phase angle constant.

3. Imbalance and mechanical faults

Imbalance is the most common source of vibration in rotating machinery. It is a very important parameter, and it must be considered carefully in the design of modern machines, especially for machines requiring a high degree of reliability and machines operating at high speeds. Mathematically, imbalance can be expressed as follows [11]:

$$\vec{U}^{\rightarrow} = m \times \vec{r}^{\rightarrow}[\text{gmm}] \tag{2}$$

where

m: unbalanced mass (g);
r: distance of unbalanced mass from the center axis (mm).

The centrifugal force imbalance that generates vibration is expressed as follows:

$$\vec{F}^{\rightarrow} = m \times \vec{r}^{\rightarrow} \times w^2[\text{N}] \tag{3}$$

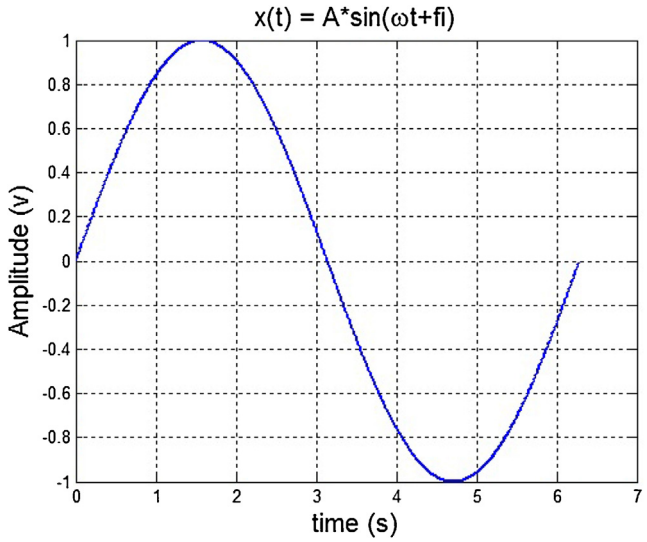

Fig. 1. Vibration signal in the time domain.

where

F: force in Newtons (N);
m: unbalanced mass (g);
r: distance of unbalanced mass from the center axis (mm);
w: speed in radians per second (rad/s).
Specific imbalance is calculated as follows:

$$\vec{e}^{\rightarrow} = \frac{m\vec{r}^{\rightarrow}}{M}[\text{g mm /kg}] = [\mu m] \tag{4}$$

The most common types of imbalance in rotating machinery are (i) static, (ii) coupled, (iii) quasi-static, and (iv) dynamic.

3.1. Static imbalance

Static imbalance is defined as the eccentricity relative to the center of gravity of a disk, caused by a point mass at a certain radial distance from the rotation center, as shown in Fig. 2. A mass-equal value, set at an angle of 180° with respect to the imbalance-causing point mass at the same radial distance, is required to restore the center of gravity to the center of rotation. Static balancing involves first resolving the forces in a plane and adding a correction mass in the same plane. Rotating parts that have many masses concentrated in only one plane can be treated as static balancing problems. If a disc has a diameter of 7–10 x its width, it is usually treated as a disk with a single plane [11]. We used the static imbalance method in this work.

4. Proposed methodology

Previously, shaft imbalance conditions were diagnosed mainly by performing vibration analysis. In this study, the authors investigated the effect of imbalance on a rotor shaft using by both vibration characteristics and a smart experimental setup based on an algorithm embedded on a FPGA. This developed method can detect and correct static imbalance.

4.1. Experimental procedure

The experiment was conducted with a smart experimental setup (Fig. 3) comprising (1) a 3-phase induction motor (0.25 cv, 4 poles, 1710 rpm); (2) variable speed controller with voltage vector control; (3) an experimental test rotor consisting of one disk measuring 90 mm in diameter and 12 mm in thickness, into which holes were punched for introducing imbalance; (4) a shaft measuring 8 mm in diameter and 250 mm in length; (5) rolling bearings; (6) ball bearings, with a reference frequency of 38,000 rpm and dynamic load of 351 kgf; (7) helical coupling, allowing an angular misalignment of 5° at a reference frequency of 25,000 rpm and rated torque of 2.3 Nm; (8) ceramic piezoelectric accelerometer with a sensitivity of 1.02 mV/(m/s) and frequency range of 0.3–15,000 Hz; (9) photoelectric sensor for monitoring the phase and frequency of

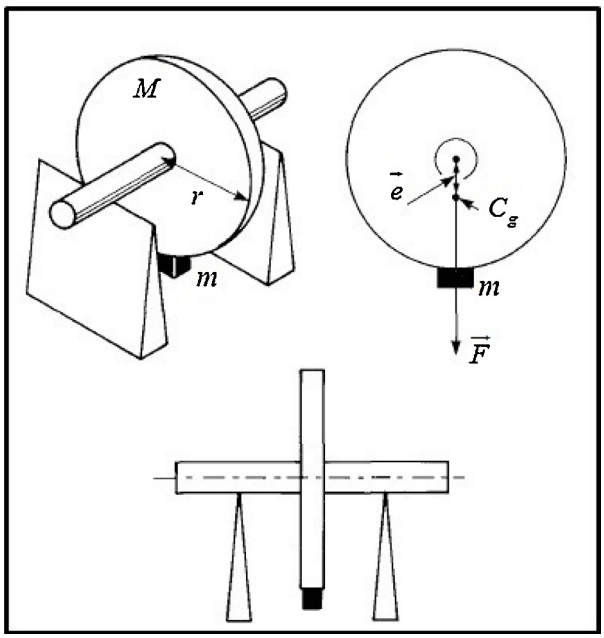

Fig. 2. Schemes of static imbalance [11].

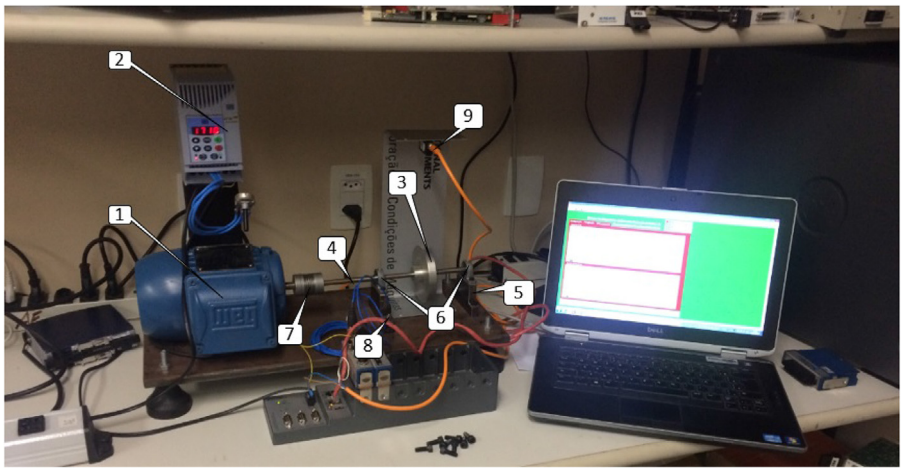

Fig. 3. Experimental setup.

shaft rotation; (10) CompactRIO hardware architecture with a real-time processor and a FPGA chip; and (11) PC running the application software in LabVIEW.

4.2. Proposed algorithm embedded in FPGA

The block diagram of the algorithm embedded in the FPGA is shown in Fig. 4. The different stages of the proposed system are discussed here.

4.3. Data processing

The hardware platform CompactRIO, based on FPGA technology, was used for the acquisition, monitoring, analysis, and processing of signals from the smart experimental setup. The CompactRIO hardware architecture combines three components: (i) a real-time processor as the system CPU; (ii) FPGA chip embedded in the structure; and (iii) space for accommodating up to eight input and output modules (accelerometer and photoelectric sensors). The model used was NI 9074, which is based on FPGA, and the physical interface with the sensors, which is required to condition the signals, perform data acquisition and analysis, and process essential calculations for the mathematical application software, served as the

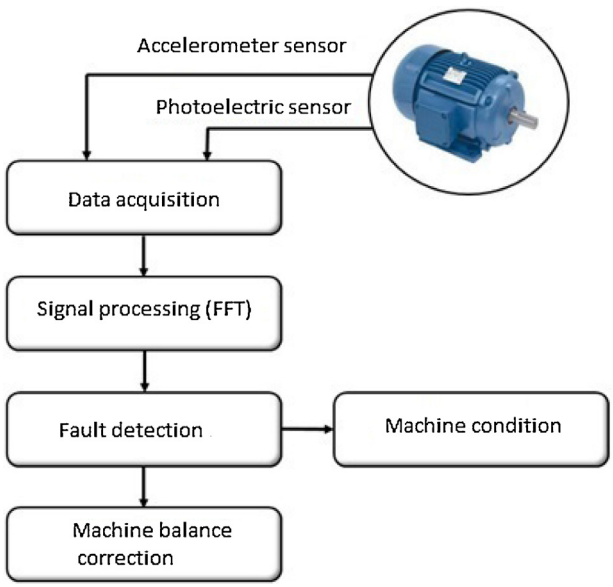

Fig. 4. Block diagram of algorithm for automatic fault imbalance detection and correction.

real-time operating system. The application software is divided into two algorithms: (i) imbalance detection and (ii) calculation of the trial mass and its position on disk for imbalance correction.

4.4. Imbalance detection algorithm

Data from the accelerometer (vibration signal) and the photoelectric sensor (speed rotor signal) are acquired for signal processing. Vibration due to the imbalance is seen as a peak in the spectrum at the vibration frequency. The vibration level and the phase of the rotational frequency of the rotor signal could be read directly from the display. Fig. 5 shows the proposed methodology, which combines the vibration and the rotational frequency signals from rotor analyses to precisely determine the motor condition according to the following procedure:

1. Acquisition of vibration and rotational frequency signals during induction motor operation;
2. Processing of vibration signal using FFT;
3. Processing of vibration and rotation frequency signals in the time domain to determine the phase angle between the signals;
4. Determining whether the motor is balanced or unbalanced from the results of the above analyses (steps 2 and 3);
5. Determining the trial mass and its position for correcting imbalance if any.

4.5. Imbalance correction algorithm

The imbalance correction algorithm used herein is based on vector diagram calculations for single-plane balancing. The magnitude and angular position of the correction mass can be determined by representing vectorially, as shown in Fig. 6.

1. A vector $\vec{V_0}$is drawn representing the initial imbalance. The length of $\vec{V_0}$is equal to the vibration amplitude, and its direction is given by the phase angle, as shown in Fig. 6a.
2. Another vector $\vec{V_1}$is drawn representing the amplitude and phase measured with the trial mass mounted, as shown in Fig. 6b.
3. The tips of vectors $\vec{V_0}$ and $\vec{V_1}$ are joined by means of a third vector $\vec{V_T}$, which is marked so that it indicates the direction from $\vec{V_0}$ to $\vec{V_1}$, as shown in Fig. 6c. This vector represents the effect of the trial mass alone.
4. A vector is drawn parallel to vector $\vec{V_T}$ with the same amplitude and direction but starting at the origin. This vector is also called $\vec{V_T}$, as shown in Fig. 6d.
5. The vector $\vec{V_0}$ is continued through the origin in the direction opposite to that of $\vec{V_0}$. This vector is called $\vec{V_C}$, and it represents the position and magnitude of the mass required to counteract the original imbalance, as shown in Fig. 6e.
6. If we assume that the vibration amplitude is proportional to the unbalanced mass, we obtain the relationship

$$\frac{M_T}{\vec{V_T}} = \frac{M_C}{\vec{V_C}} = \frac{M_0}{\vec{V_0}} \tag{5}$$

$$M_C \Rightarrow M_0 = \frac{|V_0|}{|V_T|} \times M_T \tag{6}$$

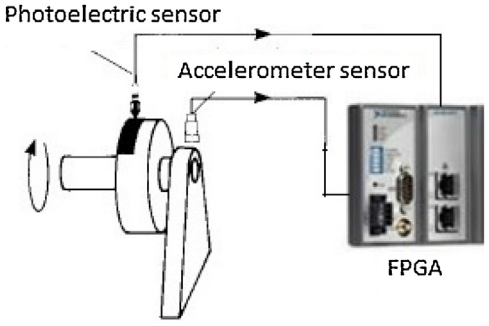

Fig. 5. Acquisition of vibration and rotational frequency signals.

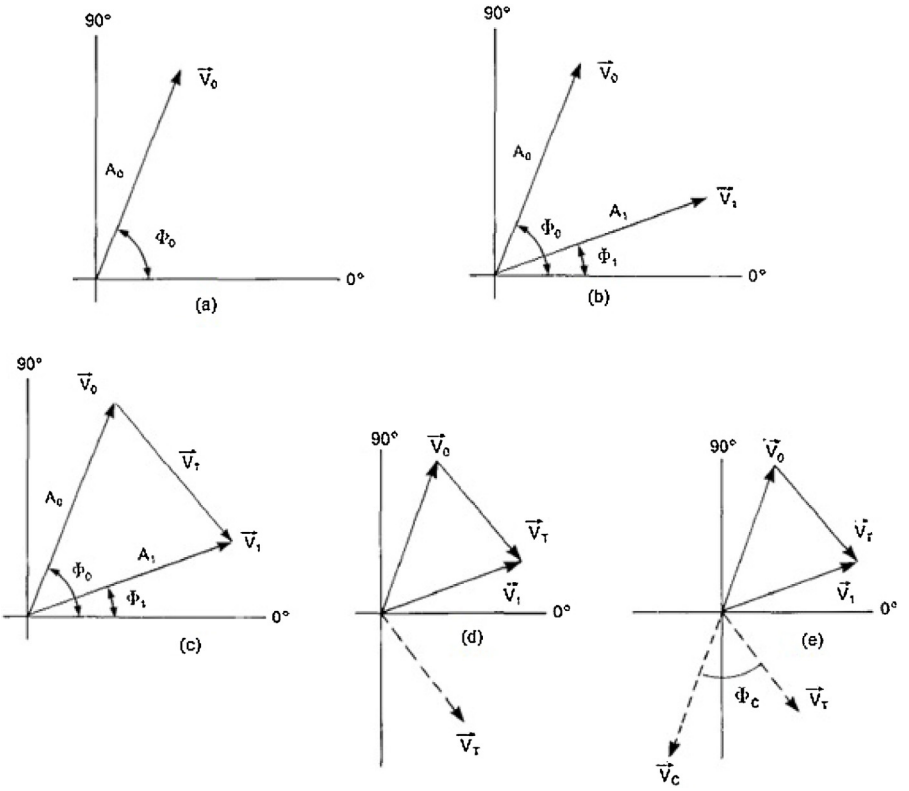

Fig. 6. Vector diagram calculations: (a) vector of initial imbalance; (b) vector of measured amplitude and phase; (c) third vector representing effect of trial mass; (d) vector parallel; and (e) vector of position and magnitude of mass [11].

Eq. (6) allows us to determine the value of the compensating mass, M_C.

7. The position of the mass relative to the position of the trial mass can be determined from the vector diagram by using Eq. (7)

$$\phi_C = \phi_T + \phi_0 + 180^0 \tag{7}$$

The calculated angle is measured from the position marked on the rotor indicating the point where the trial mass was mounted. If it is a positive angle, it is measured in the direction of rotation. A negative angle is measured in the opposite sense.

The described algorithms were developed in LabVIEW real-time software and later embedded in the reconfigurable FPGA [19–22], as shown in Fig. 7.

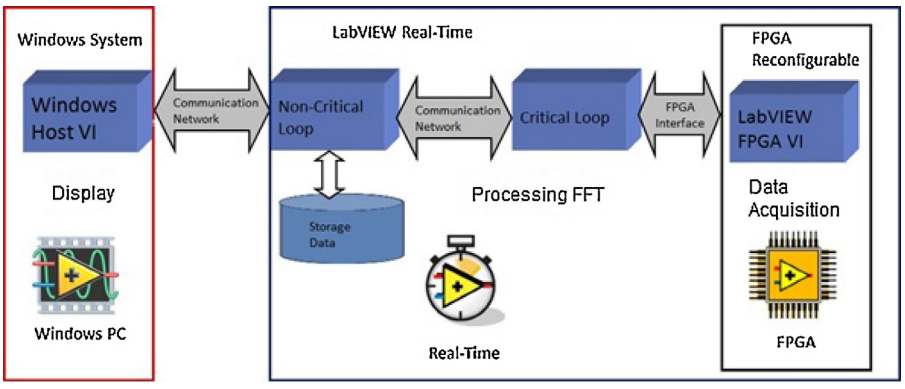

Fig. 7. Block diagram of implementation in FPGA.

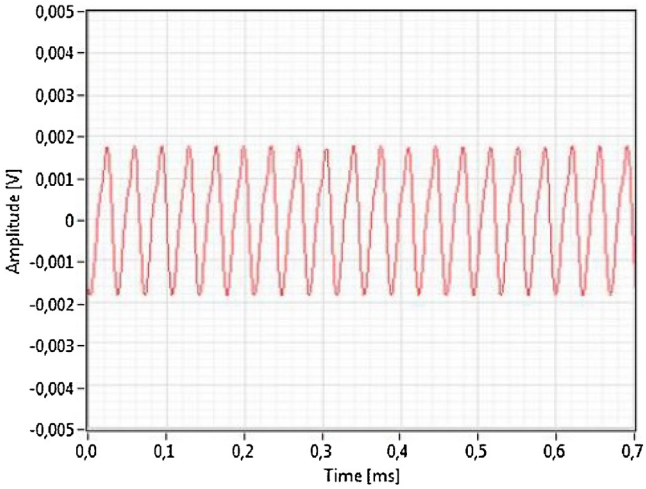

Fig. 8. Photoelectric sensor signal with balanced condition.

5. Results and analysis

The induction motor was operated at a constant speed of 28.5 Hz (1710 rpm). The vibration and rotational frequency signals of the system were recorded by an accelerometer (vibration signal) placed along the vertical direction and a photoelectric sensor (rotational speed signal) placed next to the disk.

The experiments were first performed with the balanced disk. The required imbalance was then introduced in the rotor shaft by adding a trial mass on the disk, as explained in the previous section. Experimental studies confirmed that rotor imbalance creates a vibration of frequency equal to the rotational speed and amplitude proportional to the amount of imbalance [12,13]. A series of tests, described hereinafter, were performed to focus on the relevant information in the spectrum and to discriminate the imbalance fault component.

5.1. Machine reference running balanced

In the first trial, the machine was operated without adding any mass to the disk and was therefore considered balanced. Fig. 8 shows the signal acquired by the photoelectric sensor, which was used to determine both the engine rotation frequency and the lag angle of the vibration signal.

Fig. 9 shows the time-domain vibration signal obtained by the accelerometer sensor for an unflawed, balanced rotor. The signal's peak amplitude was approximately 0.50 mV. For this balanced condition, the phase angle between the photoelectric sensor signal and the accelerometer would be equal to zero.

Fig. 10 shows the FFT result, which can be used to determine the magnitude of the signal in the frequency domain. The data contained in the vibration spectrum are processed by the system to identify imbalance failures. The signal of interest is given by the motor rotation frequency (28.5 Hz); no imbalance is detected, and the signal magnitude is 0.20 mV.

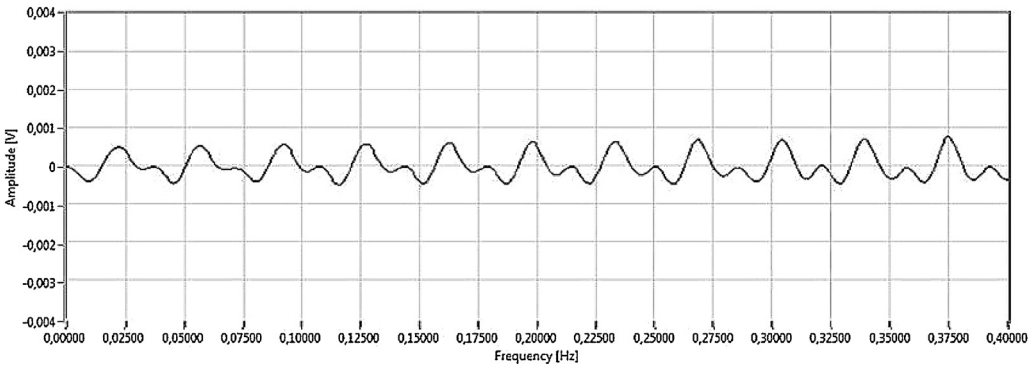

Fig. 9. Accelerometer sensor signal with balanced condition.

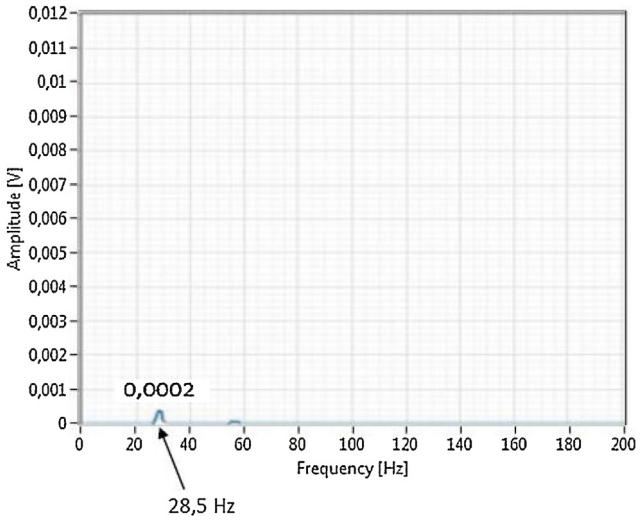

Fig. 10. Vibration spectrum signal with balanced condition.

5.2. Machine running with one mass attached

To perform imbalance fault simulation, a trial mass of pre-determined weight was introduced, as shown in Fig. 11. In the first experiment, a mass of 0.006 kg was attached to the rotor shaft disc. The imbalance thus created produced a mechanical vibration in the machine's structure.

Fig. 12 shows the time-domain vibration signal of the faulty unbalanced machine; the peak amplitude signal increased from 0.50 to 5.5 mV. This imbalance produced an increase in the machine's vibration level. In this unbalanced condition, the phase angle between the signals of the photoelectric sensor and the accelerometer was calculated to be approximately 8.5°.

Fig. 13 shows the spectrum of the vibration motor signal with a test mass. The signal of interest is given by the motor rotation frequency (28.5 Hz); an imbalance fault was detected in terms of an increase in the spectrum amplitude (from 0.20 to 5.6 mV).

5.3. Machine operation with two trial masses attached

To validate imbalance detection by using the vibration spectrum, a final experiment was performed by attaching two unbalancing masses of 0.006 kg each to the rotor shaft disc. As shown in Fig. 14, the magnitude of the vibration spectrum is 11.2 mV (an increase of approximately 56 times compared to the vibration spectrum of the balanced machine shown in Fig. 10).

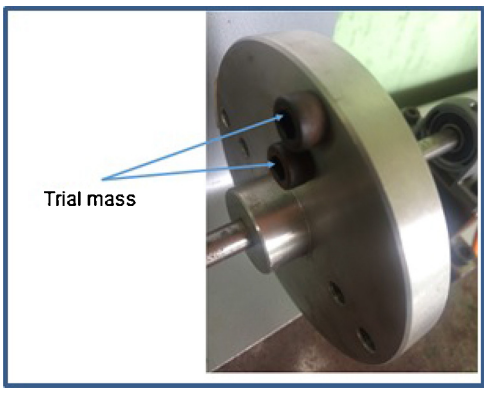

Fig. 11. Rotor shaft disc with trial mass.

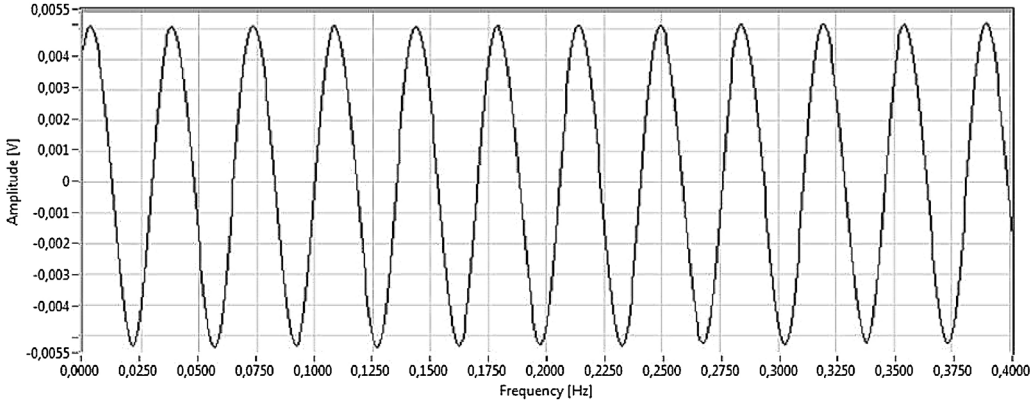

Fig. 12. Vibration signal with one trial mass.

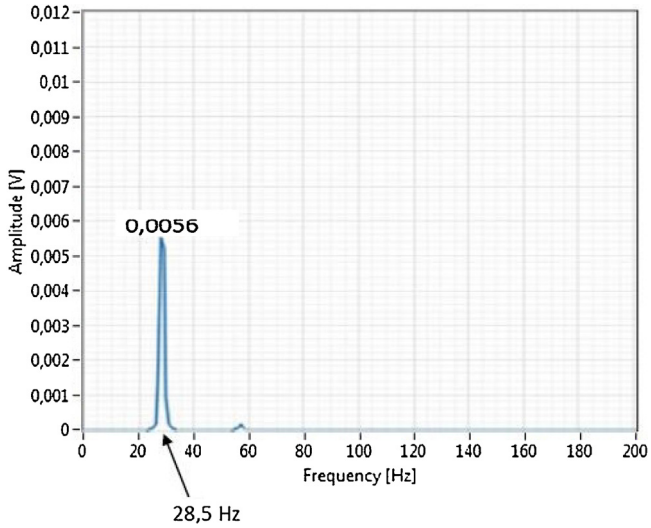

Fig. 13. Vibration spectrum measured by accelerometer with one unbalancing mass attached to the rotor shaft disc.

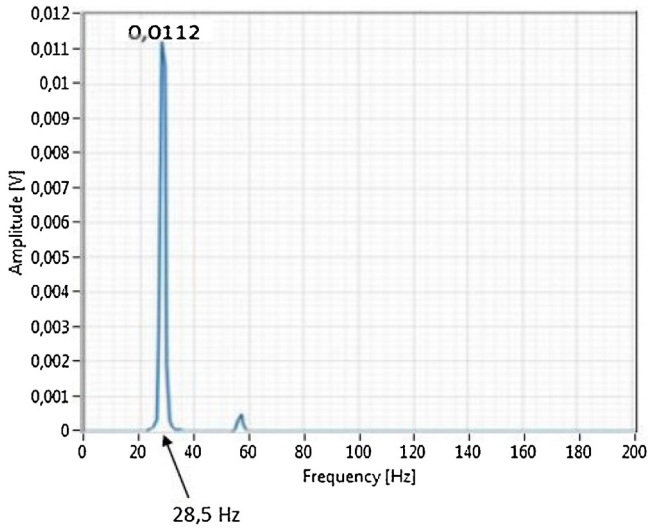

Fig. 14. Vibration spectrum measured by accelerometer with two unbalancing masses attached to the rotor shaft disc.

5.4. Balancing of shaft rotor

We implemented the proposed imbalance correction algorithm after identifying the correlation between imbalance and increase in the vibration amplitude.

To determine the values of the correction angle (ϕ_c) and the correction mass (Mc), the values of the phase angle and magnitude from V0 and V1 must be calculated. During the balancing process, two pieces of data are logged in the system memory: (i) Vector V0, referred to as the initial vibration, and (ii) Vector V1, referred to as the loading of trial masses. Once V0 and V1 have been calculated and the weight of the trial mass has been input to the software, we can calculate the correction mass and its position on the rotor shaft disc.

In addition, we conducted additional experiments for validating the proposed procedure by proving its effectiveness in balancing the system. Table 1 show four experiments in which different masses were used as imbalance masses and trial masses.

We chose the results obtained in Experiment 3, Table 1, to validate the imbalance correction process (inserting a new correction mass positioned on the disc axis) using the proposed system.

The correction process includes removing the 0.0055 kg test mass and inserting a 0.0039 kg correction mass at 86.3° (as calculated by the system) in the direction of motor rotation. The results of this are shown in Fig. 15, in which the vibration signals from the initial 0.006 kg mass are superimposed with those corresponding to the fixed 0.0039 kg correction mass.

6. Conclusions

The implementation of a smart experimental setup with an FPGA-based signal processor that combines vibration and FFT analyses yielded satisfactory results when performing online imbalance and mechanical fault identification in an induction motor.

For a constant motor rotation frequency (28.5 Hz), a comparison between the vibration levels in the time domain and their respective frequency spectra revealed a significant increase in amplitudes in all three tests, as machine imbalance increased.

Table 1
Experimentally obtained correction imbalance data.

	Experiment 1	Experiment 2	Experiment 3	Experiment 4
Machine speed (rpm)	1710	1710	1710	1710
Imbalance Mass, M_0 (kg)	0.003	0.0055	0.006	0.008
Imbalance Vector Vibration, V_0	0.0019	0.0043	0.0031	0.0047
Imbalance Angle, $\angle_0(^\circ)$	114.5	288	8.5	6
Trial Mass, M_T (kg)	0.0042	0.008	0.0055	0.0030
Trial Vector, V_T	0.0038	0.0072	0.0058	0.0059
Trial Angle, $\angle_T(^\circ)$	66.3	333.5	314.6	32.6
Correction Mass, M_C (kg)	0.0027	0.0065	0.0039	0.0057
Correction Angle, $\angle_C(^\circ)$	78	81.2	−86.3	77.7

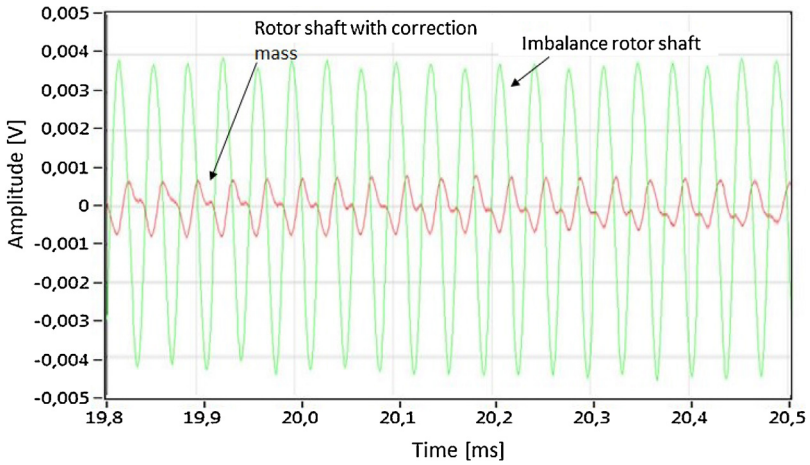

Fig. 15. The vibration signals from imbalance rotor shaft were superimposed with corresponding to the rotor shaft with correction mass.

Practical experiments using the "Smart Experimental Setup" show that adding a correction mass at the location indicated by the system effectively reduced the vibration caused by imbalance to levels similar to those of the corresponding balanced rotating machine.

The proposed smart experimental setup for vibration measurement and imbalance fault detection in rotating machinery was successfully tested and is ready for application in "real world" systems.

References

[1] S.N. Ganeriwala, B. Schwarz, M.H. Richardson, Using operating deflection shapes to detect unbalance in rotating equipment, J. Sound Vib. 43 (May (5)) (2009).
[2] S.N. Ganeriwala, L. Zhuang, M.H. Richardson, Using operating deflection shapes to detect shaft misalignment in rotating equipment, Proceedings of International Modal Analysis Conference (IMAC XXVI), February, 2008.
[3] M. Benbouzid, G. Kliman, What stator current processing based technique to use for induction motor rotor faults diagnosis, IEEE Trans. Energy Convers. 18 (June (2)) (2003) 238–244.
[4] C. Kral, T.G. Habetler, R.G. Harley, Detection of mechanical imbalances without frequency analysis, IEEE Trans. Ind. Appl. 40 (4) (2004) 1101–1106 (July/August).
[5] A.K. Verma, S. Sarangi, M.H. Kolecar, Experimental investigations of misalignment effects on rotor shaft vibration and on stator current signature, J. Fail. Anal. Prev. 14 (2) (2016) 125–138.
[6] J.Z. Szabo, Vibration diagnostic test for effect of unbalance, INES 2012-16th International Conference on Intelligent Engineering System, Lisbon, Portugal, 13-15, 2012, pp. 81–85.
[7] J. Piotrowski, Shaft Alignment Handbook, 3rd edn., CRC, New York, 2006.
[8] T.H. Patel, A.K. Darpe, Vibration response of misaligned rotor, J. Sound Vib. 325 (2009) 609–628.
[9] J.M. Bossio, G.R. Bossio, C.H. De Angelo, Angular misalignment in induction motor with flexible coupling, Proceedings of the IEEE IECON, Porto, Portugal, 3–7 November, 2009, 2016, pp. 1033–1038.
[10] R.R. Obaid, T.G. Habetler, R.M. Tallam, Detecting load unbalance and shaft misalignment using stator current in inverter-driven induction motors, Electric Machines and Drives Conference. IEMDC'03. IEEE Internacional Volume 3, 1–4 June 2003, 2003, pp. 1454–1458.
[11] M. MacCamhaoil, Static and dynamic balancing of rigid rotors, BruelKjaer (2016) 1–20 (Application note).
[12] F. Jiang, W. Li, Z. Wang, Z. Zhu, Fault severity estimation of rotating machinery based on residual signals, Adv. Mech. Eng. (2012) (ID 518468, 8 pages).
[13] H. Bendjama, S. Bouhouche, M.S. Boucherit, Application of wavelet transform for fault diagnosis in rotating machinery, Int. J. Mach. Learn. Comput. 2 (1) (2012) 82–87.
[14] J.D. Martinez-Moralez, E. Palacios, D.U. Campos-Delgado, Data fusion for multiple mechanical fault diagnosis in induction motors at variable operating conditions, Proceedings of the 7th International Conference on Electrical Engineering, Computing Science and Automatic Control, pp. 176–181, September 2010, 2016.
[15] W. Qiao, X. Gong, Imbalance fault detection of direct-drive wind turbines using generator current signals, IEEE Trans. Eergy Convers. 27 (2) (2012) 468–476.
[16] A. Kucuker, M. Bayrak, Detection of mechanical imbalances of induction motors with instantaneous power signature analysis, J. Electr. Eng. Technol. 8 (5) (2013) 1116–1121.
[17] J.J. Saucedo-Dorantes, M. Delgado-Prieto, J.A. Ortega-Redondo, R.A. Osornio-Rios, R.J. Romero-Troncoso, Multiple-Fault detection methodology based on vibration and current analysis applied to bearings in induction motors and gearboxes on the kinematic chain, Shock Vib. (2016) (art. no. 5467643).
[18] A.G. Garcia-Ramirez, R.A. Osornio-Rios, D. Granados-Lieberman, A. Garcia-Perez, R.J. Romero-Troncoso, Smart sensor for online detection of multiple-combined faults in VSD-fed induction motors, Sensors (Switzerland) 12 (9) (2012) 11989–12005.
[19] E. Cabal-Yepez, A.G. Garcia-Ramirez, R.J. Romero-Troncoso, A. Garcia-Perez, R.A. Osornio-Rios, Reconfigurable monitoring system for time-frequency analysis on industrial equipment through STFT and DWT, IEEE Trans. Ind. Inf. 9 (2) (2013) 760–771.
[20] P.K.K. Krishnaveni, Design and implementation of a system on FPGA for fault detection on industrial machines through vibration sensing, Appl. Mech. Mater. 110–116 (2012) 5351–5357.
[21] P.S. Panigrahy, P. Konar, P. Chattopadhyay, Broken bar fault detection using fused DWT-FFT in FPGA platform, 2014 International Conference on Power, Control and Embedded Systems, ICPCES 2014 (2014) (art. no. 7062819).
[22] M. Kashiwagi, C. Da Costa, M.H. Mathias, Digital systems design based on DSP algorithms in FPGA for fault identification in rotary machines, J. Mech. Ind. Res. 2 (2014) 1–5.